Article ID: 1000-7032(2022)03-0430-10

Sensitive Detection of Captopril Based on "Off-On" Carbon Dots as Fluorescent Probe

LIANG Qian[1], WANG Yu-lin[2], ZHENG Mei-qin[1], CHEN Yan-xi[1], HUANG Wen-jie[1], LI Guang-man[3], HUANG Biao[2]*

(1. *Jinshan College of Fujian Agriculture and Forestry University, Fuzhou* 350002, *China*;
2. *Fujian Agriculture and Forestry University, Fuzhou* 350002, *China*; 3. *Chongqing Customs Technical Center, Chongqing* 401147, *China*)

* *Corresponding Author, E-mail: bhuang@fafu.edu.cn*

Abstract: Fluorescent nitrogen-doped carbon dots (NCDs) were synthesized by a facile one-step microwave strategy using lemon juice and urea. The obtained NCDs show stable blue fluorescence with a high quantum yield of 53.1%. Hg^{2+} can efficiently coordinate onto the surface of NCDs by means of electrostatic interactions and remarkably quench the fluorescence of NCDs as a result of the formation of a non-fluorescent stable NCDs-Hg^{2+} complex (turn-off). Static fluorescence quenching towards Hg^{2+} is proved by the fluorescence lifetime measurements and the change of ultraviolet-visible absorption spectra. In addition, the fluorescence of NCDs-Hg^{2+} system was recovered with the addition of captopril (CAP) due to the ability of captopril to coordinate with Hg^{2+} and the formation of strong Hg^{2+}—S bond. When captopril was added, Hg^{2+} combined with captopril rather than with NCDs resulting in the remove of Hg^{2+} from the surface of NCDs and a significant fluorescence restore of NCDs was observed (turn-on). Under the optimized conditions, good linearity for detecting captopril was attained over the concentration range 0.25 – 25 μmol · L^{-1} with a detection limit of 0.17 μmol · L^{-1}. Moreover, this NCDs-based sensor was successfully applied for quantitation of captopril in tablets with satisfactory recovery.

Key words: carbon dots; fluorescence; captopril; Hg(Ⅱ)
CLC number: O482.31 **Document code**: A **DOI**: 10.37188/CJL.20210372

基于碳点的荧光探针"关-开"测定卡托普利

梁 倩[1], 王玉林[2], 郑梅琴[1], 陈艳希[1], 黄文杰[1], 李光满[3], 黄 彪[2]*

(1. 福建农林大学金山学院, 福建 福州 350002;
2. 福建农林大学, 福建 福州 350002; 3. 重庆海关技术中心, 重庆 401147)

摘要: 以柠檬汁和尿素为原料,通过一步简单的微波热解制得了含氮荧光碳点(NCDs)。所得碳点发蓝色荧光,量子产率高达53.1%。Hg^{2+}可以与NCDs表面基团络合形成非荧光的稳定化合物,导致荧光猝灭。通过荧光猝灭与寿命的关系和紫外-可见光谱的变化情况得出猝灭应属静态猝灭。另外,卡托普利的加入可以使NCDs荧光得以恢复,这是因为Hg^{2+}与卡托普利的成键作用强于NCDs,卡托普利的加入使Hg^{2+}脱离NCDs表面,荧光得以恢复。在最优化的实验条件下,卡托普利的检测范围是0.25 ~ 25 μmol · L^{-1},检出限为0.17 μmol · L^{-1}。该探针成功地用于卡托普利片剂中有效成分的测试并取得了满意的效果。

关 键 词: 碳点; 荧光; 卡托普利; Hg(Ⅱ)

收稿日期: 2021-11-29; **修订日期**: 2021-12-24
基金项目: 国家重点研发计划(2017YFD0601006); 福建省教育厅项目(kz180414,JT180846)资助
Supported by National Key Research and Development Program of China (2017YFD0601006); Education Project of Fujian Provincial Department (kz180414, JT180846)

1 Introduction

Captopril((2S)-1-[(2S)-2-methyl-3-sulfanyl-propanoyl] pyrrolidine-2-carboxylic acid, CAP) is an orally active inhibitor of angiotensin-converting enzyme and is widely used in the management of hypertension and congestive heart failure[1-2]. It may also be useful in preventing and treating congestive heart failure[3-4]. During the metabolic pathway, it is converted to a disulfide compound, which is eliminated together with unchanged captopril (40% – 60%) in urine. With the increasing of clinical application, some adverse effects are reported for captopril, such as cough, hematemesis, proteinuria, renal injury[5-6]. Therefore, a facile, rapid, sensitive and selective detection of captopril in biological and pharmaceutical preparation samples is desired and has attracted a great deal of attention[7]. Methods used for quantitation of captopril include high-performance liquid chromatography (HPLC) with mass spectrometric[8], atomicabsorption/emission spectrometry[9], fluorescence[5,10-14], chemiluminescence[7,15] and electrochemical techniques[15-18]. However, the above methods are expensive, time-consuming or requiring complex mathematic dealing. In the present work, we developed a new method for the determination of captopril based on the fluorescence "off-on" of NCDs.

Carbon dots have attracted tremendous attentions owing to their captivating properties[19-20], such as excellent photo-stability, favorable biocompatibility, and good water solubility[21-22]. Carbon dots using in a broad range of promising applications have been demonstrated in bioimaging[23], medical diagnosis[24], catalysis[25], photovoltaic devices[26] and sensor[27-29] especially for sensor application[30-31]. Many methods have been proposed to prepare NCDs during the last decade, such as chemical ablation, electrochemical carbonization, laser ablation, hydrothermal/solvothermal treatment[32]. In contrast, microwave irradiation of organic compounds is a rapid and low-cost method to synthesize NCDs[14,33]. In this study, we report a microwave strategy for the preparation of nitrogen-doped carbon dots(NCDs) by using the lemon juice and urea. The obtained NCDs show blue fluoresces with a high quantum yield of 53.1%. We found the introduced Hg^{2+} may cause fluorescence "turn-off" of the NCDs. Moreover, the NCDs-Hg^{2+} system can also be conveniently employed as a fluorescent "turn-on" probe for highly sensitive and selective detection of captopril with a low limit of detection (LOD) of 0.17 $\mu mol \cdot L^{-1}$ and a wider linear detection range of 0.25 – 25 $\mu mol \cdot L^{-1}$. Cumulatively, our present work demonstrates the efficacy of NCDs as an effective fluorescent probe for potential applications in biomedical applications.

2 Experiment

2.1 Materials and Instruments

All the experiments were carried out using analytical grade without further purification. Captopril and quinine sulfate were purchased from Aladdin Ltd. (Shanghai, China). $Fe_2(SO_4)_3$, KCl, $CaCl_2$, $BaCl_2$, $AlCl_3$, $HgCl_2$, $MgCl_2$, $MnCl_2$, $ZnCl_2$, $CuCl_2$, $CoCl_2$, $CdCl_2$, $AgNO_3$, NaCl, $Pb(NO_3)_2$, $NiCl_2$, urea were obtained from the Sinopharm Chemical Reagent Co., Ltd. (Shanghai, China). The water used here was purified through a Kertone-mini water purification system throughout the experiments. The lemons were purchased from a local supermarket.

UV-Vis absorption spectra were recorded on a UV-2600 UV-Vis spectrophotometer (shinadzu, Japan). Fluorescence emission spectra were recorded by a FS5 fluorescence spectrophotometer (Edinburgh, UK). X-ray photo-electron spectroscopy (XPS) was performed on a Thermo ESCALAB 250XI electron spectrometer equipped with Al Kα X-ray radiation ($h\nu$ = 1 486.6 eV) as the source for excitation. Transmission electron microscopy (TEM) was performed on a Zeiss Libra 200 FE transmission electron microscope at an acceleration voltage of 200 kV. Fourier transform infrared spectroscopy (FTIR) experiments were recorded on a AVATAR360 FTIR spectrometer in the form of KBr pellets.

2.2 Synthesis of Nitrogen Doped Carbon Dots

The NCDs were synthesized by microwave method. In brief, we squeeze the lemon and filter out the pulp to get the lemon juice. 2 g urea was

dissolved in 10 mL lemon juice to achieve solution and then the solution was heated in microwave oven for 15 min operating at 700 W. After the beaker had cooled down to room temperature, the obtained blank solid powder was dissolved with 20 mL water. The supernatant was filtered with 0.22 μm filter membrane to remove the large carbon dots and then dialyzed against ultra-pure water through a dialysis membrane (Molecule weight cut off is 1 000 u) for 24 h. Finally, the yellow NCDs solution was obtained.

2.3 Fluorescence Sensing of Captopril

For detection of CAP, different amounts of CAP (1 mmol · L^{-1}) were added into the mixture solution of NCDs (100 μL) and Hg^{2+} (100 μL, 1 mmol · L^{-1}). The final concentration of CAP ranged from 0 to 200 μmol · L^{-1}. All samples were incubated for 45 min at room temperature and recorded under excitation at 413 nm to obtain the fluorescence spectra.

2.4 Quantum Yield of NCDs

Quinine sulfate dispersed in 0.1 mol · L^{-1} H_2SO_4 (Quantum yield is 0.58) was used as the standard. The quantum yield was calculated with the following equation:

$$Y_u = Y_s \cdot \frac{F_u}{F_s} \cdot \frac{A_s}{A_u}, \quad (1)$$

where Y is quantum yield, F is integrated area of emission, and A is the absorbance at the excited wavelength of the sample, respectively. The subscripted "s" refers to the referenced fluorophore with known quantum yield and "u" refers as the samples for the determination of quantum yield.

2.5 Determination of Captopril in Tablets

The tablets were finely powdered. An amount of this powder, equivalent to about 10.9 mg of CAP was accurately weighed and shaken with 20 mL of distilled water in a water-bath at 50 ℃ for 10 min. The mass of CAP was calculated with the equation (2):

$$m = cVM, \quad (2)$$

where c is the concentration, and M is molecular weight of CAP. After cooling, the solution was transfered into a 50 mL calibrated flask, the residue was washed several times and the solution diluted with water to the mark to obtain a solution of 1 mmol · L^{-1}.

3 Results and Discussion

3.1 Characterization of NCDs

The TEM image (Fig. 1(a)) shows that the as-prepared NCDs were well dispersed. The diameter distribution of the NCDs rangs from 1.0 nm to 7.0 nm and the average diameter of NCDs is 3.7 nm (inset of Fig. 1(a)), which is well consistent with the NCDs reported[34]. FTIR spectrum was used to identify the functional groups present on NCDs. As shown in Fig. 1(b), there existed N—H, O—H, C═O, C—O and C—H groups on the surface of the NCDs. Specifically, the stretching vibration of —OH/—NH was located at 3 440 cm^{-1}. The stretching vibrations of —CH were located at 2 923 cm^{-1} and 2 850 cm^{-1}. The band at 1 713 cm^{-1} was attributed to the C═O stretching vibration. The band at 1 400 cm^{-1} could be ascribed to —CH bending vibration. While the band at 1 200 was ascribed to C—O stretching vibration[35].

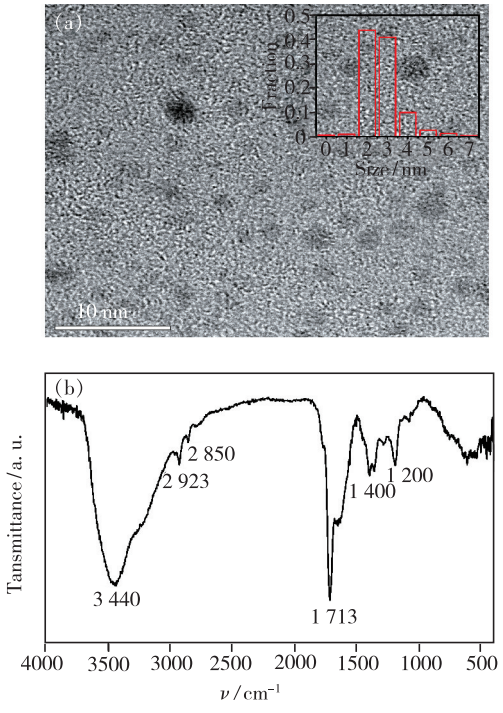

Fig. 1 (a) TEM image of the NCDs (inset: the diameter distribution of the NCDs). (b) FTIR spectrum.

Moreover, XPS was used to analyze the elemental composition and the chemical bonds of the

prepared NCDs. As shown in Fig. 2(a), the survey XPS spectra revealed three typical peaks of C 1s at 285 eV, N 1s at 400 eV, O 1s at 531 eV and the corresponding content of each element. The high-resolution spectra of C 1s in Fig. 2(b) exhibit three main peaks(C—C 284.7 eV, C—O 286 eV, C ═O 288 eV). The spectra of N 1s in the NCDs reveal the presence of N—H(399.6 eV) and C—N(400.3 eV) bonds(Fig. 2(c)), while that of O 1s(Fig. 2(d)) displays two peaks(531.4 eV and 532.1 eV), which could be attributed to C—O and C ═O groups, respectively[36].

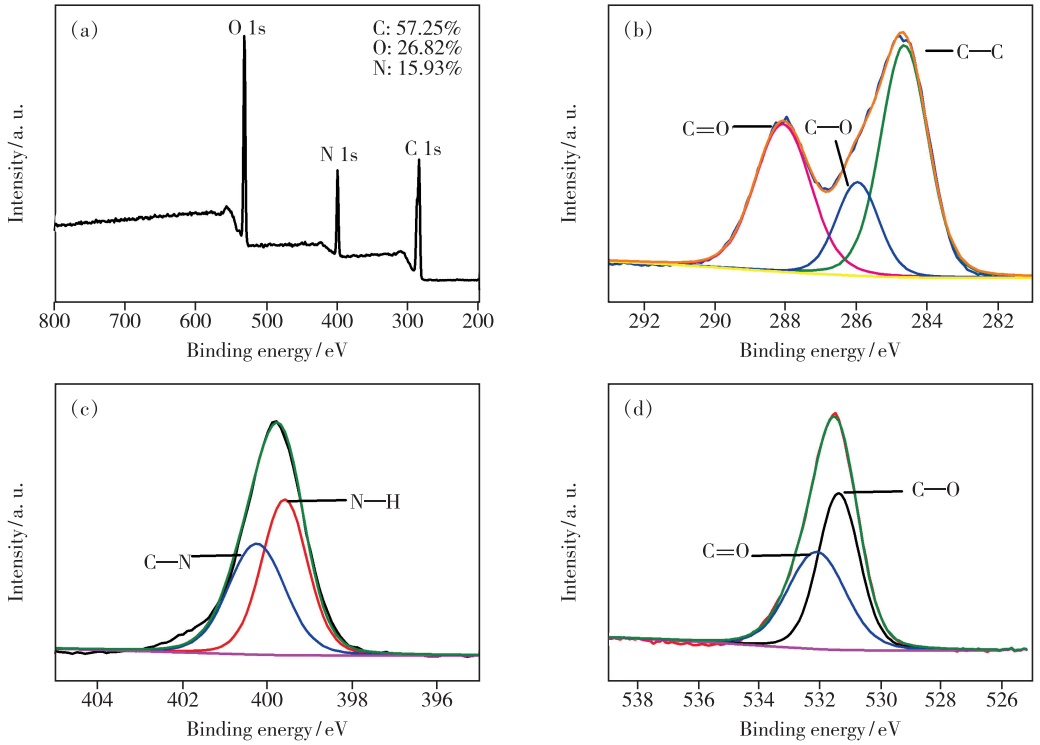

Fig. 2 (a) Full-scan XPS spectrum of the NCDs. (b) C 1s XPS spectra. (c) N 1s XPS spectra. (d) O 1s XPS spectra.

The UV-Vis absorption spectrum of the NCDs showed that there was a shoulder peak at 272 nm and an absorption band at 328 nm and 414 nm(Fig. 3). The shoulder peak at 272 nm was attributed to the π-π* transitions of the aromatic C ═C bonds. While the absorption at 328 nm and 413 nm were from n-π* transitions[37].

The maximum emission was available at 536 nm with maximum excitation at 413 nm(Fig. 3). Thus, the 413 nm was chosen as the optimal excitation wavelength for the following detection experiments. The above result indicated that highly fluorescent NCDs were successfully synthesized. In order to further explore the fluorescence properties of the as-prepared NCDs, the quantum yield and the effects of different extraneous factors on the fluorescence intensity of the NCDs were investigated. Under the excitation of 360 nm, the quantum yield of the NCDs was measured to be 53.1% using quinine sulfate in 0.1 mol · L^{-1} H_2SO_4 as a reference.

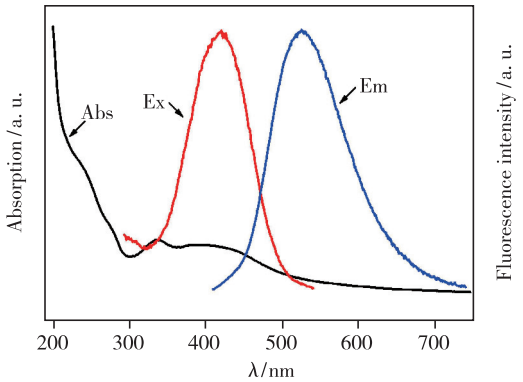

Fig. 3 UV-Vis absorption(Abs) and fluorescence emission spectra(Ex: excitation) of the NCDs

3.2 Fluorescence Stability of NCDs

The ionic strength and pH value were investigated to conform the stability of the NCDs. The effect of ionic strength on fluorescence intensity of synthesized

NCDs is investigated by incorporating 0 – 3 mol · L^{-1} NaCl in the solution of NCDs (Fig. S1 (a)). The result reveals that fluorescence intensity of NCDs is constant in high ionic strength. The pH value of NCDs was studied over the range from 2.0 to 11.0 (Fig. S1 (b)). The fluorescence intensity changing in the pH range 2 – 7 was nearly closed to each other, while higher pH value reduced the fluorescence intensity. This phenomenon may be attributed to the deprotonation of carboxyl group and amino group on the NCDs surface. These results showed that the fluorescence intensity of the NCDs was stable under broad acidic condition and neutral condition. At low pH, the active sites will be reduced for the protonation of the functional groups on the surface of the NCDs. While under alkaline conditions, the Hg^{2+} may combine with the —OH to form $Hg(OH)_2$. Moreover, the dispersal environment for CAP is nearly neutral. Consequently, pH 6.0 was chosen in the next experiments.

3.3 Effect on Fluorescence by Hg^{2+}

To demonstrate the feasibility and specificity of the NCDs for Hg^{2+} detection, the sensing experiment was performed with different metal ions under the same condition. The plot depicts that the NCDs solution show strong quenching in fluorescence emission spectra in presence of 50 μmol · L^{-1} Hg^{2+}, while other metal ions have virtually no influence on the fluorescence detection of Hg^{2+} (Fig. 4 (a)). These results clearly demonstrate that the proposed NCDs possess outstanding selectivity for Hg^{2+} and can serve as novel fluorescence sensor for highly selective and reliable Hg^{2+} monitoring.

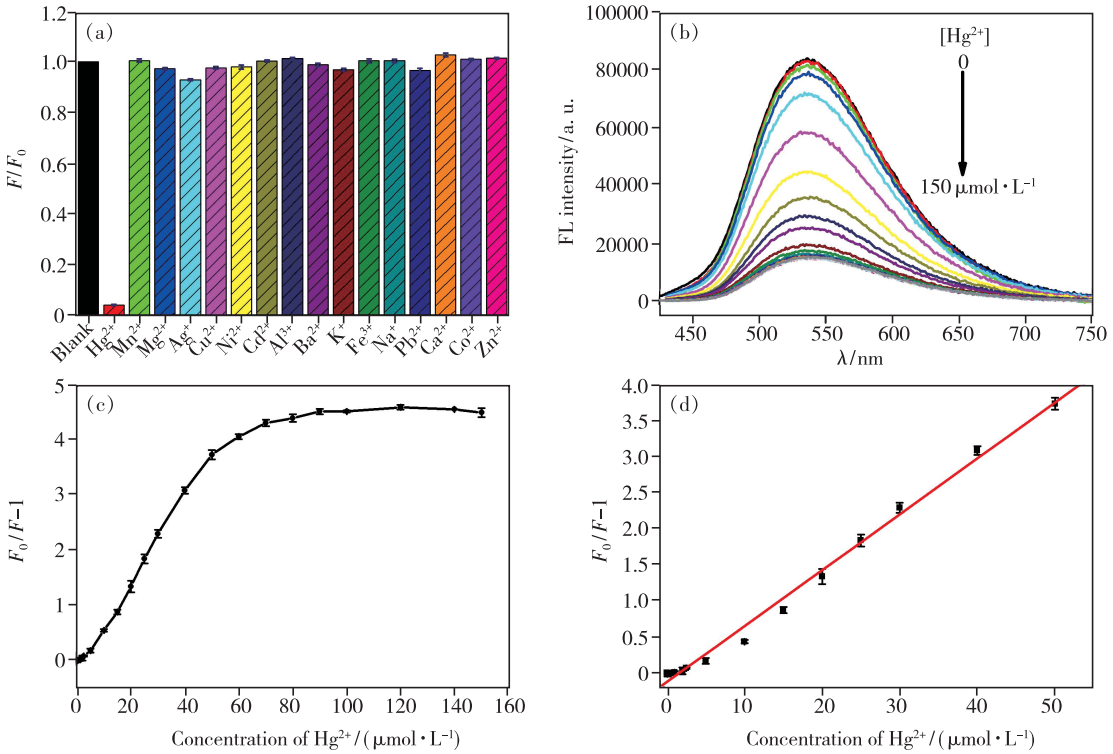

Fig. 4 (a) Selectivity of the NCDs for Hg^{2+} (the concentration of Hg^{2+} and other metal cations were 50 μmol · L^{-1}). (b) Emission spectra of the NCDs in the present of various concentrations of Hg^{2+} (from top to bottom, 0, 0.02, 0.2, 1, 2, 5, 10, 20, 30, 50, 60, 80, 100, 120, 140, 150 μmol · L^{-1}). (c) The plot of $F_0/F-1$ and the concentration of Hg^{2+}. (d) The linear plot of $F_0/F-1$ and the concentration of Hg^{2+}.

The titration experiment was conducted by adding Hg^{2+} aqueous solution at different concentrations to NCDs solution. As shown in Fig. 4 (b), upon the addition of Hg^{2+}, the fluorescence intensity of NCDs was gradually quenched upon the addition of Hg^{2+}. It may be due to the electrostatic interactions between Hg^{2+} and the carboxylate or hydroxyl groups on the surface of NCDs. It is clear that the

value of $F_0/F-1$ declined gradually with the enhancement of Hg^{2+} concentration, and reached a platform when a higher Hg^{2+} concentration(>80 μmol · L^{-1}) was used (Fig. 4(c)). Meanwhile, the fluorescence quenching at 536 nm was in a distinct linear relationship with the Hg^{2+} concentration in the range of 0.50 – 50 μmol · L^{-1} (Fig. 4 (d)). The linear correlation could be described by the linear regression equation $F_0/F-1=-0.1241+0.07719C_{Hg^{2+}}$, with a correlation coefficient of 0.993 (R^2) and a limit of detection was calculated to be 0.21 μmol · L^{-1}.

The quenching mechanism process was studied in order to investigate the reasons for its high selectivity of Hg^{2+}. In order to obtain further insight into the mechanism of quenching, we investigated the fluorescence lifetime of the NCDs with and without the Hg^{2+}. Fluorescence lifetime measurement is the most definitive method to distinguish static and dynamic quenching[38]. For static quenching, the fluorescence lifetime does not change ($\tau_0/\tau=1$), where τ_0 and τ are the fluorescence lifetime in the absence and presence of quencher, respectively. In contrast, for dynamic quenching, $F_0/F=\tau_0/\tau$, and the lifetime decreases on addition of the quencher. The fluorescence lifetime spectra (Fig. S2) and the fluorescence intensity decay were fitted to a three exponential decay function (Tab. S1). The average fluorescence lifetime (τ_0) of pure NCDs is calculated to be 7.13 ns. With gradual addition of Hg^{2+} 25 μmol · L^{-1} and 50 μmol · L^{-1} respectively, the average lifetime of NCDs decays to 6.88 ns (τ_1) ($\tau_0/\tau_1=1.04$) and 6.63 ns (τ_2) ($\tau_0/\tau_2=1.07$). The ratio of the fluorescence intensity of the pure NCDs (F_0) and the presence of Hg^{2+} is $F_0/F_1=2.18$, $F_0/F_2=3.40$ respectively. F_0, F_1 and F_2 are fluorescence intensity in the absence and presence different concentration of Hg^{2+} respectively. The ratio of the average fluorescence lifetime of NCDs was more close to 1.0, ruling out the dynamic quenching mechanism[10]. Moreover, upon addition of 50 μmol · L^{-1} Hg^{2+}, the absorption centered at 337 nm becomes weak, suggesting the formation of non-fluorescent stable NCDs-Hg^{2+} complex *via* the the electrostatic interactions between Hg^{2+} and NCDs (Fig. 5). These results indicate that the static quenching between NCDs and Hg^{2+} cations is possible[39].

3.4 Feasibility and Sensitivity of NCDs Detection of CAP in Deionized Water Sample

To research the feasibility of NCDs-Hg^{2+} fluorescence probe for CAP detection, 60 μmol · L^{-1} CAP is added into NCDs-Hg^{2+} system. The quenched fluorescence of the NCDs-Hg^{2+} complex was recovered within 45 min (Fig. S3 and Fig. S4), and then the fluorescence intensity remained stable. Furthermore, the restoration of the UV-Vis absorption centered at 337 nm indicates the release of NCDs (Fig. 5). This phenomenon may be due to the strong binding preference between Hg^{2+} and thiol groups. Hg^{2+} is dissociated from the surface of NCDs through the formation of Hg^{2+}—S bond, which leads to the complete recovery of the emission of NCDs (Fig. 6)[40-41].

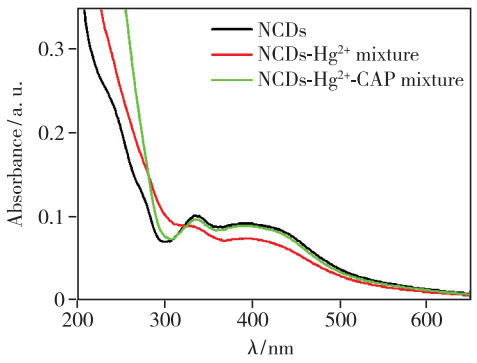

Fig. 5 UV-Vis absorption spectra of NCDs (black), the mixture of NCDs and Hg^{2+} (red), and the mixture of NCDs, Hg^{2+} and captopril (green).

To further investigate the sensitivity of NCDs-Hg^{2+} system to CAP, different concentrations of CAP in the range of 0 – 200 μmol · L^{-1} were added into NCDs-Hg^{2+} system containing 30 μmol · L^{-1} Hg^{2+}. For the original NCDs-Hg^{2+} solution, there is only a very weak emission at 536 nm owing to the quenching effect from Hg^{2+} cations (Fig. 7 (a)). The fluorescence intensity at 536 nm of NCDs-Hg^{2+} system is gradually strengthened with the increasing concentration of CAP from 0 to 120 μmol · L^{-1} and then flattened, revealing that the NCDs-Hg^{2+} system is sensitive to CAP. Moreover, no spectral shift of

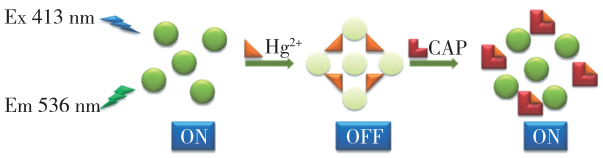

Fig. 6 The detecting pathway for Hg^{2+} and CAP based on the fluorescence switching of NCDs

the emission band is observed. The relationship between the fluorescence intensity at 536 nm of NCDs-Hg^{2+} system and the concentration of CAP is shown in Fig. 7(b). The fluorescence is completely restored in the presence of 120 μmol · L^{-1} CAP. The fluorescence intensity enhancement can also be analyzed by the Stern-Volmer equation: $F_2/F_1 = 1 + K_{sv1}[Q_1]$, where F_1 and F_2 are the fluorescence intensity at 536 nm of NCDs-Hg^{2+} system in the absence and presence of CAP, respectively, K_{sv1} is the Stern-Volmer constant and $[Q_1]$ is the concentration of CAP. As shown in Fig. 7(c), a linear plot for the quantitative analysis of CAP can be fitted between the F_2/F_1 and the concentration of CAP over a range of 0.25 – 25 μmol · L^{-1}. The linear correlation could be described by the linear regression equation $F_2/F_1 = 1.0976 + 0.0165C_{CAP}$, with a correlation coefficient of 0.991 (R^2) and a limit of detection was calculated to be 0.17 μmol · L^{-1}. These results suggested that such NCDs-Hg^{2+} system as a fluorescent turn-on probe exhibits superior sensitivity for CAP, wide linear response range and high possibility for the quantitative detection of CAP. Some representative probes for sensing CAP are summarized in Tab. 1 for comparison. The NCDs-Hg^{2+} fluorescent sensor for CAP detection not only exhibits better or comparable performance, but also is cheaper and easier to prepare.

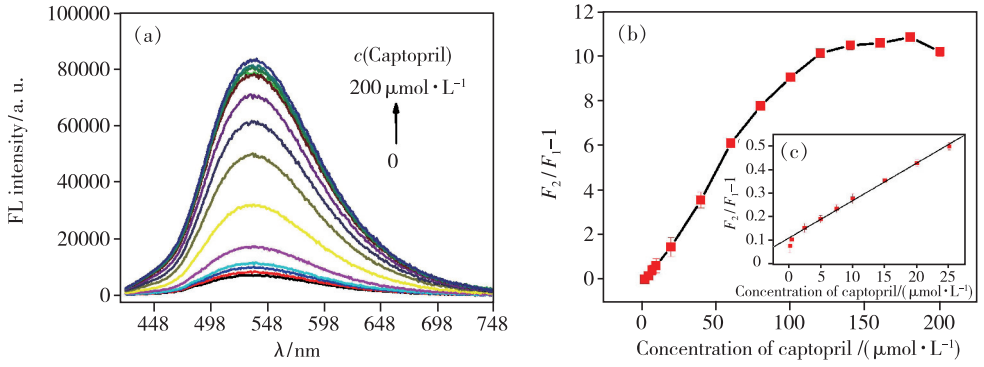

Fig. 7 (a) Emission spectra of the NCDs -Hg^{2+} system in the present of various concentrations of CAP (from bottom to top, 0, 0.25, 0.5, 2.5, 5, 7.5, 10, 20, 40, 60, 80, 100, 120, 140, 160, 180, 200 μmol · L^{-1}). (b) The plot of F_2/F_1-1 and the concentration of CAP. (c) The linear plot of F_2/F_1 – 1 and the concentration of CAP.

Tab. 1 Comparison of different probes for the sensing of captopril

Methods	Probes	Linear range/ (μmol · L^{-1})	Detection limit/ (μmol · L^{-1})	Reference
Cyclic voltammetry	Graphite screen printed electrodes	0 – 800	4.27	[7]
Fluorimetry	Gold nanoparticles- fluorescein isothiocyanate	0.09 – 2.9	0.012	[12]
Fluorimetry	Graphene oxide	0.5 – 10.5	0.157 8	[13]
Fluorimetry	Boron and nitrogen codoped carbon quantum dots	0.1 – 60	0.03	[14]
Cyclic voltammetry	Chlorpromazine modified glassy carbon	8 – 1 000	4.8	[15]
Differential pulse voltammetry	Cobalt-5-nitrolsalophen modified carbon paste	4.0 – 110	1.1	[16]
Cyclic voltammetry	Multi-wall carbon nanotubes-hexacyanoferrate(Ⅱ)	0.5 – 600	0.2	[17]
Square wave voltammetry	Boron doped diamond	0.09 – 0.46	0.165	[18]
Fluorimetry	NCDs-Hg^{2+}	0.25 – 25	0.17	This work

3.5 Interference Studies

In order to apply the proposed method to the analysis of pharmaceutical dosage forms, the influence of commonly used excipients and additives was studied by preparing NCDs-Hg^{2+} solutions containing captopril and the foreign compound. As shown in Fig. 8, no interference was found for mannose, fructose, dextrin, polyethylene glycol (PEG), starch, maltose, glucose, sucrose, microcrystalline cellulose (MCC), sorbitol and lactose. Hence, the proposed method may be considered as sufficiently selective.

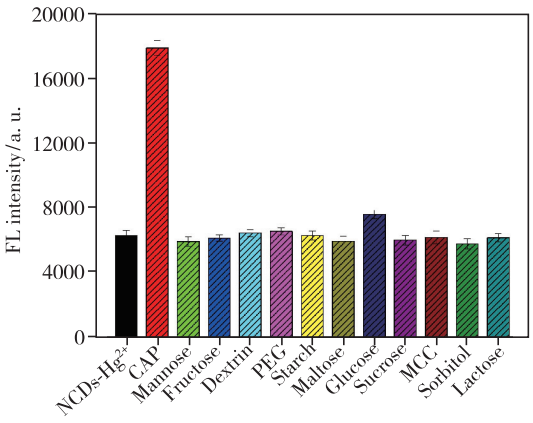

Fig. 8 Selectivity of the NCDs-Hg^{2+} system toward CAP (the concentration of CAP and other excipients and additives were both 50 μmol · L^{-1})

The proposed method was applied to the determination of captopril in tablets. The results labeled and found amount are summarized in Tab. 2. There were no significant differences between labeled amount and those obtained by the proposed method. The recoveries ranged from 96.84% to 101.2%. These results indicated the method is feasible in the detection of CAP.

Tab. 2 Determination of captopril in tablets and recovery experiments

Number	Labeled amount/ (μmol · L^{-1})	Found amount/ (μmol · L^{-1})	Recovery/% (n = 5)
1	5	5.06	101.20
2	15	14.68	97.87
3	25	24.21	96.84

4 Conclusion

In summary, a simple, low-cost and one-pot microwave method was adopted to prepare NCDs from lemon juice and urea. The obtained NCDs with a fluorescence quantum yield of 53.1% had strong fluorescence emission at 536 nm, good water solubility and high stability. In addition, the Hg^{2+} could coordinate onto NCDs and lead to significant fluorescence quenching due to the static quenching. Because of that captopril has stronger binding preference toward Hg^{2+} than NCDs due to the formation of Hg^{2+}—S bond, a significant fluorescence enhancement was observed when captopril was added into NCDs-Hg^{2+} system. Thus, the NCDs were employed for the "off-on" probe to the detection of Hg^{2+} and captopril in aqueous solution at pH = 6.0. The assay system showed sensitive and selective detection of Hg^{2+} and captopril with detection limits 0.21 μmol · L^{-1} and 0.17 μmol · L^{-1}, respectively. Our fluorescent sensor also successfully detects captopril in tablets with satisfactory recovery.

Supplementary Information and Response Letter are available for this paper at: http://cjl.lightpublishing.cn/thesisDetails#10.37188/CJL.20210372.

References:

[1] ZHU L, LU N, LIU D X. Hospital internet of things system design and captopril treatment of hypertension nursing intervention [J]. *Microprocess. Microsy.*, 2021, 82: 103922.

[2] ROOSTALU U, THISTED L, SKYTTE J L, *et al.* Effect of captopril on post-infarction remodelling visualized by light sheet microscopy and echocardiography [J]. *Sci. Rep.*, 2021, 11(1): 5241-1-13.

[3] VASCONCELOS D L M, DE SOUSA F F, DA SILVA FILHO J G, *et al.* Raman spectroscopy of captopril crystals under low-temperature conditions [J]. *Spectrochim. Acta A Mol. Biomol. Spectrosc.*, 2020, 243: 118734-1-19.

[4] WANG Y, LI Y L, RUAN S Y, *et al.* Antihypertensive effect of rapeseed peptides and their potential in improving the effectiveness of captopril [J]. *J. Sci. Food. Agric.*, 2020, 101(7): 3049-3055.

[5] 龙星宇,陈福南,邓茂. 高效液相色谱-柱后化学发光法检测人体尿液中的卡托普利[J]. 分析化学, 2012,40(7):1076-1080.
LONG X Y,CHEN F N,DENG M. Determination of captopril in human urine samples by high performance liquid chromatography coupled to post-column chemiluminesence detection[J]. *Chin. J. Anal. Chem.*, 2012,40(7):1076-1080. (in Chinese)

[6] LONG S Y,CHEN Z P,CHEN Y C,*et al.* Quantitative detection of captopril in tablet and blood plasma samples by the combination of surface-enhanced Raman spectroscopy with multiplicative effects model[J]. *J. Raman Spectrosc.*, 2015, 46(7):605-609.

[7] AREIAS M C C,TOH H S,LEE P T,*et al.* Voltammetric detection of captopril on graphite screen printed electrodes[J]. *Electroanalysis*, 2016,28(4):742-748.

[8] VANCEA S,IMRE S,DONÁTH N G,*et al.* Determination of free captopril in human plasma by liquid chromatography with mass spectrometry detection[J]. *Talanta*, 2009,79(2):436-441.

[9] RESANO M,GARCÍA-RUIZ E,ARAMENDÍA M,*et al.* Solid sampling-graphite furnace atomic absorption spectrometry for Hg monitoring in soils. Performance as a quantitative and as a screening method[J]. *J. Anal. At. Spectrom.*, 2005, 20(12):1374-1380.

[10] LIU Y,LIU C Y,ZHANG Z Y. Synthesis of highly luminescent graphitized carbon dots and the application in the Hg^{2+} detection[J]. *Appl. Surf. Sci.*, 2012,263:481-485.

[11] HORMOZI-NEZHADA M R,BAGHERI H,BOHLOUL A,*et al.* Highly sensitive turn-on fluorescent detection of captopril based on energy transfer between fluorescein isothiocyanate and gold nanoparticles[J]. *J. Lumin.*, 2013,134:874-879.

[12] SHI Y,PENG J,MENG X Y,*et al.* Turn-on fluorescent detection of captopril in urine samples based on hydrophilic hydroxypropyl β-cyclodextrin polymer[J]. *Anal. Bioanal. Chem.*, 2018,410(28):7373-7384.

[13] SUN X Y,LIU B,LI S C,*et al.* Reusable fluorescent sensor for captopril based on energy transfer from photoluminescent graphene oxide self-assembly multilayers to silver nanoparticles[J]. *Spectrochim. Acta A Mol. Biomol. Spectrosc.*, 2016,161(5):33-38.

[14] JIANG X H,QIN D M,MO G C,*et al.* Facile preparation of boron and nitrogen codoped green emission carbon quantum dots for detection of permanganate and captopril[J]. *Anal. Chem.*, 2019,91(17):11455-11460.

[15] ENSAFI A A,ARABZADEH A. A new sensor for electrochemical determination of captopril using chlorpromazine as a mediator at a glassy carbon electrode[J]. *J. Anal. Chem.*, 2012,67(5):486-496.

[16] SHAHROKHIAN S,KARIMI M,KHAJEHSHARIFI H. Carbon-paste electrode modified with cobalt-5-nitrolsalophen as a sensitive voltammetric sensor for detection of captopril[J]. *Sens. Actuators B Chem.*, 2005,109(2):278-284.

[17] REZAEI B,DAMIRI S. Voltammetric behavior of multi-walled carbon nanotubes modified electrode-hexacyanoferrate(Ⅱ) electrocatalyst system as a sensor for determination of captopril[J]. *Sens. Actuators B Chem.*, 2008,134(1):324-331.

[18] VITORETI A B F,ABRAHÃO O,DA SILVA GOMES R A,*et al.* Electroanalytical determination of captopril in pharmaceutical formulations using boron-doped diamond electrodes[J]. *Int. J. Electrochem. Sci.*, 2014,9:1044-1054.

[19] ZUO P L,LU X H,SUN Z G,*et al.* A review on syntheses,properties,characterization and bioanalytical applications of fluorescent carbon dots[J]. *Microchim. Acta*, 2016,183(2):519-542.

[20] HOU J Y,LI J L,SUN J C,*et al.* Nitrogen-doped photoluminescent carbon nanospheres:green,simple synthesis *via* hair and application as a sensor for Hg^{2+} ions[J]. *RSC Adv.*, 2014,4(70):37342-37348.

[21] THULASI S,KATHIRAVAN A,ASHA JHONSI M. Fluorescent carbon dots derived from vehicle exhaust soot and sensing of tartrazine in soft drinks[J]. *ACS Omega*, 2020,5(12):7025-7031.

[22] FENG T,AI X Z,AN G H,*et al.* Charge-convertible carbon dots for imaging-guided drug delivery with enhanced *in vivo* cancer therapeutic efficiency[J]. *ACS Nano*, 2016,10(4):4410-4420.

[23] SCHROER Z S,WU Y F,XING Y Q,*et al.* Nitrogen-sulfur-doped graphene quantum dots with metal ion-resistance for bioimaging[J]. *ACS Appl. Nano Mater.*, 2019,2(11):6858-6865.

[24] FENG Y J,ZHONG D,MIAO H,*et al.* Carbon dots derived from rose flowers for tetracycline sensing[J]. *Talanta*, 2015, 140:128-133.

[25] JU J,CHEN W. *In situ* growth of surfactant-free gold nanoparticles on nitrogen-doped graphene quantum dots for electrochemical detection of hydrogen peroxide in biological environments[J]. *Anal. Chem.*, 2015,87(3):1903-1910.

[26] KUMAR A, KUMARI A, SHARMA G, *et al.* Carbon quantum dots and reduced graphene oxide modified self-assembled S @ C_3N_4/B@ C_3N_4 metal-free nano-photocatalyst for high performance degradation of chloramphenicol [J]. *J. Mol. Liq.*, 2020, 300: 112356-1-14.

[27] JU J, ZHANG R Z, CHEN W. Photochemical deposition of surface-clean silver nanoparticles on nitrogen-doped graphene quantum dots for sensitive colorimetric detection of glutathione [J]. *Sens. Actuators* B *Chem.*, 2016, 228: 66-73.

[28] 王诗琪, 涂雨菲, 刘之晓, 等. 微波法制备掺氮碳点及其用作探针检测铁离子 [J]. 发光学报, 2019, 40(6): 751-757.
WANG S Q, TU Y F, LIU Z X, *et al.* Microwave synthesis of nitrogen-doped carbon dots and its application in detection of ferric ions [J]. *Chin. J. Lumin.*, 2019, 40(6): 751-757. (in Chinese)

[29] 汪雪琴, 洪碧云, 杨旋, 等. 壳聚糖碳点的水热法制备及其对金属离子的选择性研究 [J]. 发光学报, 2019, 40(3): 289-297.
WANG X Q, HONG B Y, YANG X, *et al.* Hydrothermal preparation of chitosan carbon dots and their selectivity to metal ions [J]. *Chin. J. Lumin.*, 2019, 40(3): 289-297. (in Chinese)

[30] WANG C X, PAN C W, WEI X R, *et al.* Emissive carbon dots derived from natural liquid fuels and its biological sensing for copper ions [J]. *Talanta*, 2020, 208: 120375-1-9.

[31] WANG G, GUO Q L, CHEN D, *et al.* Facile and highly effective synthesis of controllable lattice sulfur-doped graphene quantum dots *via* hydrothermal treatment of durian [J]. *ACS Appl. Mater. Interfaces*, 2018, 10(6): 5750-5759.

[32] 张震, 曲丹, 安丽, 等. 荧光碳点的制备、发光机理及应用 [J]. 发光学报, 2021, 42(8): 1125-1140.
ZHANG Z, QU D, AN L, *et al.* Preparation, luminescence mechanism and application of fluorescent carbon dots [J]. *Chin. J. Lumin.*, 2021, 42(8): 1125-1140. (in Chinese)

[33] CAO M, LI Y, ZHAO Y Z, *et al.* A novel method for the preparation of solvent-free, microwave-assisted and nitrogen-doped carbon dots as fluorescent probes for chromium(Ⅵ) detection and bioimaging [J]. *RSC Adv.*, 2019, 9(15): 8230-8238.

[34] TIAN T, HE Y, GE Y L, *et al.* One-pot synthesis of boron and nitrogen co-doped carbon dots as the fluorescence probe for dopamine based on the redox reaction between Cr(Ⅵ) and dopamine [J]. *Sens. Actuators* B *Chem.*, 2016, 240: 1265-1271.

[35] LIN L P, RONG M C, LU S S, *et al.* A facile synthesis of highly luminescent nitrogen-doped graphene quantum dots for the detection of 2,4,6-trinitrophenol in aqueous solution [J]. *Nanoscale*, 2015, 7(5): 1872-1878.

[36] YE Q H, YAN F Y, SHI D C, *et al.* N,B-doped carbon dots as a sensitive fluorescence probe for Hg^{2+} ions and 2,4,6-trinitrophenol detection for bioimaging [J]. *J. Photochem. Photobiol.* B, 2016, 162: 1-13.

[37] LIU Y H, ZHAO Y Y, ZHANG Y Y. One-step green synthesized fluorescent carbon nanodots from bamboo leaves for copper(Ⅱ) ion detection [J]. *Sens. Actuators* B: *Chem.*, 2014, 196: 647-652.

[38] ZHANG Y, CUI P P, ZHANG F, *et al.* Fluorescent probes for "off-on" highly sensitive detection of Hg^{2+} and L-cysteine based on nitrogen-doped carbon dots [J]. *Talanta*, 2016, 152: 288-300.

[39] YU J, SONG N, ZHANG Y K, *et al.* Green preparation of carbon dots by Jinhua bergamot for sensitive and selective fluorescent detection of Hg^{2+} and Fe^{3+} [J]. *Sens. Actuators* B: *Chem.*, 2015, 214: 29-35.

[40] ZONG J, YANG X L, TRINCHI A, *et al.* Carbon dots as fluorescent probes for "off-on" detection of Cu^{2+} and L-cysteine in aqueous solution [J]. *Biosens. Bioelectron.*, 2014, 51: 330-335.

[41] XU L F, HAO J J, YI T, *et al.* Probing the mechanism of the interaction between L-cysteine-capped-CdTe quantum dots and Hg^{2+} using capillary electrophoresis with ensemble techniques [J]. *Electrophoresis*, 2015, 36(6): 859-866.

梁倩(1984 -), 女, 河北石家庄人, 博士, 讲师, 2020 年于福建农林大学获得博士学位, 主要从事碳量子点荧光材料合成及传感的研究。
E-mail: lqfafu@163.com

黄彪(1966 -), 男, 福建古田县人, 博士, 教授, 博士生导师, 2004 年于南京林业大学获得博士学位, 主要从事生物质化学工程、生物质材料与能源等领域的研究。
E-mail: bhuang@fafu.edu.cn